

Acoustic detection of larval fish aggregations in Galician waters (NW Spain)

Eva García-Seoane^{1,6,*}, Gustavo Álvarez-Colombo², Joan Miquel³,
José María Rodríguez⁴, Carlos Guevara-Fletcher⁵, Paula Álvarez⁵, Fran Saborido-Rey¹

¹Instituto de Investigaciones Marinas (CSIC), C/Eduardo Cabello 6, 36208 Vigo, Pontevedra, Spain

²Instituto Nacional de Investigación y Desarrollo Pesquero (INIDEP), Paseo Victoria Ocampo 1, CC 175, B7602HSA Mar del Plata, Argentina

³Instituto Español de Oceanografía, Centre Oceanogràfic de les Balears (IEO), Moll de Ponent, s/n, PO Box 291, 07080 Palma de Mallorca, Spain

⁴Instituto Español de Oceanografía, Centro Oceanográfico de Gijón (IEO), Avda. Príncipe de Asturias 70Bis, 33213 Gijón, Asturias, Spain

⁵AZTI-Tecnalia, Marine Research Division, C/ Herrera Kaia, Portualdeaz.g. 20110 Pasaia, Gipuzkoa, Spain

⁶Present address: Instituto Português do Mar e Atmosfera (IPMA), Av. Brasília, s/n, 1449-006 Lisboa, Portugal

ABSTRACT: An acoustic study was conducted on the Galician shelf (NW Spain) during late winter 2012 to detect and assess larval fish abundance. An echo sounder operating with 18, 38, 70, 120 and 200 kHz split-beam, hull-mounted transducers was employed. We analysed the acoustic records in order to describe vertical and horizontal distribution patterns of larval fish aggregations. Regressions between acoustic backscattered energy and density of the most abundant species (*Micromesistius poutassou*) indicated that larvae with a swimbladder incremented notably the acoustic response at 38, 70 and 120 kHz. However, the predicted acoustic resonance at larval size and depth shows that the frequency of 120 kHz was likely ineffective in detecting fish larvae. The contribution of zooplankton (fish larvae excluded) to total scattering was negligible, even at the higher frequencies, except for several groups of fluid-like zooplankton, such as chaetognaths and polychaetes. Horizontal and vertical distributions of acoustic backscattering also indicated that larval fish aggregations can be detected in Galician waters with acoustics and suggest that this technique is a useful tool for overcoming difficulties associated with larval ecology and fish recruitment studies.

KEY WORDS: Acoustics · Fish larvae · Zooplankton · Frequency response · Galician shelf

—Resale or republication not permitted without written consent of the publisher—

INTRODUCTION

The embryonic and larval stages in fish have important ecological and evolutionary functions. For many species, they represent an effective means of dispersal that can extend the range of a population and mix the gene pool (Cowen & Sponaugle 2009, Pusack et al. 2014). They are also interactive components of the pelagic ecosystem that can, for example, temporarily reduce local zooplankton populations so that the potential for competition for food is height-

ened (Nielsen & Munk 1998, Beaugrand et al. 2003). However, one of the most important reasons for studying the early life stages of fishes is that the year-class strength of fish populations is determined at these stages, shortly after depletion of the yolk-sac, when larvae must find suitable amounts and types of plankton prey (Hjort 1914, Houde 2008). Predicting recruitment represents a challenge in fisheries science, and our ability to do that remains poor. To estimate larval fish abundance is a complex and difficult process, involving elaborate and expensive sur-

veys, but such surveys provide detailed descriptions of phenological relationships affecting recruitment (Hare 2014). Additionally, understanding dispersal distance is important for a variety of reasons, including fisheries management, effective design of marine protected areas, and control of invasive species (Cowen et al. 2006, Becker et al. 2007, Almany et al. 2009, Cowen & Sponaugle 2009, Aiken & Navarrete 2011, Le Corre et al. 2012). Long time-series of egg and larval abundance and distribution data facilitate a spatial comparison of spawning habitats (Van der Lingen & Huggett 2003, Ibaibarriaga et al. 2007, Álvarez & Chifflet 2012) and play an important role in fishery management of many species through applying egg and larval production methods to estimate fish stock biomass (Motos et al. 1996, Stratoudakis et al. 2004, Lo et al. 2009).

To sample fish larvae effectively, proper nets and efficient sampling designs are required. These conventional sampling methods, however, suffer from many well-known drawbacks; they include those related to sampling devices, larval size and larval behaviour, such as net avoidance, extrusion and clogging (Barkley 1972, Wiebe et al. 1982, Leslie & Timmins 1989, Johnson & Morse 1994, Hernandez et al. 2011), and problems associated with the nature of sequential sampling. The high degree of patchiness and low mean density, typically shown by larval distribution contribute to increase variance, uncertainty and reduces precision of abundance estimations (Lo et al. 2009). Methods that overcome such limitations are required (e.g. acoustic and molecular techniques). The virtues of echo-sounder records are the speed of areal coverage and the real-time data presentation of the echogram.

The acoustic method is often used for abundance estimation of juvenile and adult fish of commercially important stocks worldwide (Misund 1997). Also, plankton has been studied acoustically for many years, and the growing importance of this field is now evident (MacLennan & Holliday 1996). The increased use of acoustics may help to elucidate some problems related to the estimation of larval fish abundance (Rudstam et al. 2002, Godø et al. 2014). However, to date, few fish larval studies applying acoustic techniques have been carried out. In order to assess *Engraulis encrasicolus* larval distribution in the Strait of Sicily, Bonanno et al. (2006) divided the acoustic signal according to the percentages of zooplankton and fish larvae found in biological samples. Rudstam et al. (2002) concluded that it is difficult to exclude noise or invertebrate targets in abundance estimates of fish larvae smaller than 15 mm, although

they reported reliable abundance estimates of fish as small as 15 mm.

In the case of fish with small-volume swimbladders, e.g. fish larvae and mesopelagic fish, the likelihood of acoustic detection is increased at low frequencies due to resonance scattering (Godø et al. 2009). Using theoretical models, Miyashita (2003) estimated higher sound scattering levels at 38 kHz than at 120 kHz for *Engraulis japonicus* post-larvae with inflated swimbladders during the night. Recently, on the Argentinean shelf, Álvarez-Colombo et al. (2011) detected *Merluccius hubbsi* aggregations acoustically, in coincidence with the development of larval functional swimbladders at about 4 mm total length. These authors demonstrated that the high intensity levels of acoustic backscattering recorded from these aggregations at 38 kHz were due to resonance scattering, showing the potential of the acoustic method during fish assessment surveys applied to the detection and spatial distribution analysis of larval fish aggregations. This innovative use of acoustics should be contrasted not only in other fish species but also in different geographical areas.

The aim of this study was to test the hypothesis that larval fish aggregations may be detected and assessed by acoustic techniques in waters of the Iberian Peninsula. We analysed the acoustic records in order to estimate abundance and to describe horizontal and vertical distribution patterns of larval fish aggregations. We tested our hypothesis on the Galician shelf (NW Spain) during the course of a holistic research project on hake recruitment. This region is located within the northern border of the seasonal coastal upwelling that extends along the eastern coasts of the North Atlantic, and whose intensity depends on the North Atlantic anti-cyclonic eddy (McClain et al. 1986). The upwelling is associated with high primary productivity which determines the structure of the pelagic and benthic food webs (Fariña et al. 1997). This produces one of the most important and intensive fisheries in the European Union, making this area the most fishing-dependent region in Europe (Surís-Regueiro & Santiago 2014).

MATERIALS AND METHODS

Biological sampling

Within the frame of the research project on hake recruitment ecology, a specific cruise (Cramer0312) was carried out off the NW Iberian peninsula (Fig. 1) in late winter 2012 (from February 28 to March 13),

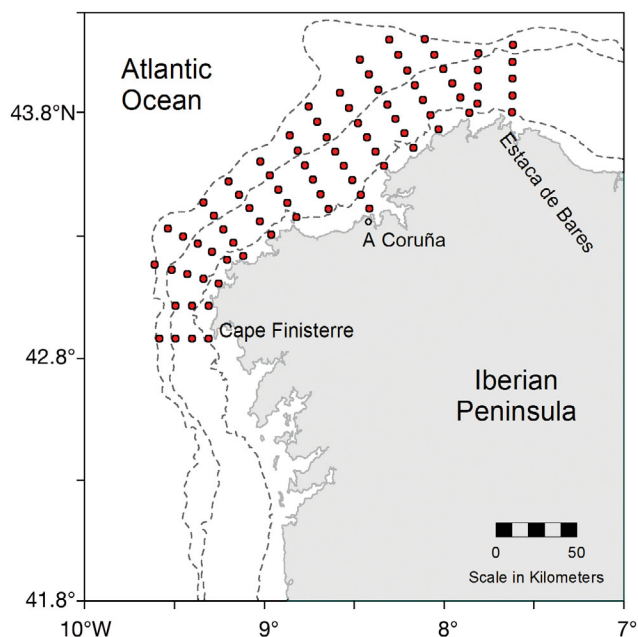


Fig. 1. Map of the Galician shelf (NW Iberian Peninsula). The sampling stations were represented by red points, outlining a total of 15 transects. Isobaths are for depths of 100, 200 and 500 m

during the main spawning peak of this species in the region. The sampling design covered the area from Finisterre to Estaca de Bares, from around 40 m to 500 m depth. Considering that hake presents highly aggregated spawning behavior, adaptive cluster sampling was implemented starting with a grid of 80 stations arranged in 15 transects perpendicular to the coastline. The distance between stations and transects was 4 n mile and 8 n mile, respectively (Fig. 1). Four stations were not included in the study because of sampling errors.

At the sampling grid stations, zooplankton was collected at 5 fixed depth strata (0–20, 20–40, 40–60, 60–100 and 100–200 m depth) with a multiple opening/closing MultiNet MiDi, 50 × 50 cm aperture (MultiNet Hydro-Bios Apparatebau), equipped with 5 nets of 200 μm mesh size. The net, programmed to open/close at the predefined depths, was towed obliquely, from 200 m depth or from ~ 10 m above the bottom, at shallower stations. The tow speed was of 2.5–3 knots and the retrieval rate of the net was of 20 m min^{-1} . The volume of water filtered in each stratum was measured by an electronic flowmeter located in the mouth of the net. Samples were immediately preserved in a 5% solution of buffered formalin and seawater.

In the laboratory, all fish larvae were sorted from the samples and identified to the lowest taxonomic

level possible. Larvae of the most abundant taxa (those with ≥ 20 larvae caught, both day and night) were photographed with a Nikon Act-2u camera and subsequently measured for standard length using the ImageJ 1.45s image analysis software (available at <http://rsb.info.nih.gov/>). Larval lengths were not corrected for shrinkage (Theilacker 1980).

Zooplankton samples (fish larvae excluded) collected with the Multinet Midi were analysed using semi-automated zooplankton counting and classification methods. For each zooplankton sample, the whole volume was measured and a sub-sample of 5 ml was taken and stained. The stained samples were digitized using an EPSON V750 PRO scanner (VueScan Professional Edition 8.5.02 software) generating an image resolution of 2400 dpi. After that, images were analysed using ZooImage free software (licensed under GNU/GPL) to obtain mesozooplankton abundance and size (Bachiller & Fernandes 2011, Bachiller et al. 2012). Each zooplankton individual was automatically counted and measured. Mesozooplankton counts were standardized by the software to number of individuals per m^3 . Detailed analyses of larval fish and zooplankton distribution and abundance from this survey are found in Rodríguez et al. (2015a,b).

Acoustic data

During the survey, acoustic backscattering was continuously recorded by an EK60 echo sounder operating with 18, 38, 70, 120 and 200 kHz split-beam, hull-mounted transducers. A beam width of 7° was common for all frequencies, except 18 kHz, with an 11° beam. A transmitted pulse length of 1.024 ms was employed in all frequencies. The acoustic system was calibrated before the survey following the standard target method (Foote et al. 1987) with a 38.1 mm diameter tungsten-carbide sphere positioned under the extended dropkeel.

The acoustic signals were analysed and integrated by the post-processing system Echoview v4.20. The volume backscatter threshold (S_v , dB re 1 m^{-1}) was -75 dB. In order to analyse the relationship between the volume scattering intensities and net catches, the sampling gear trajectory was plotted in the echogram from depth data obtained with a ScanmarTM pressure sensor attached to the MultiNet sampler. Real-time depth data registered by this sensor were transmitted by acoustic telemetry to hull-mounted hydrophones, allowing us to monitor the net's path and to send the datagram via a LAN port to the ER-60 echo sounder. A specific software routine (*El Gregoriano*, devel-

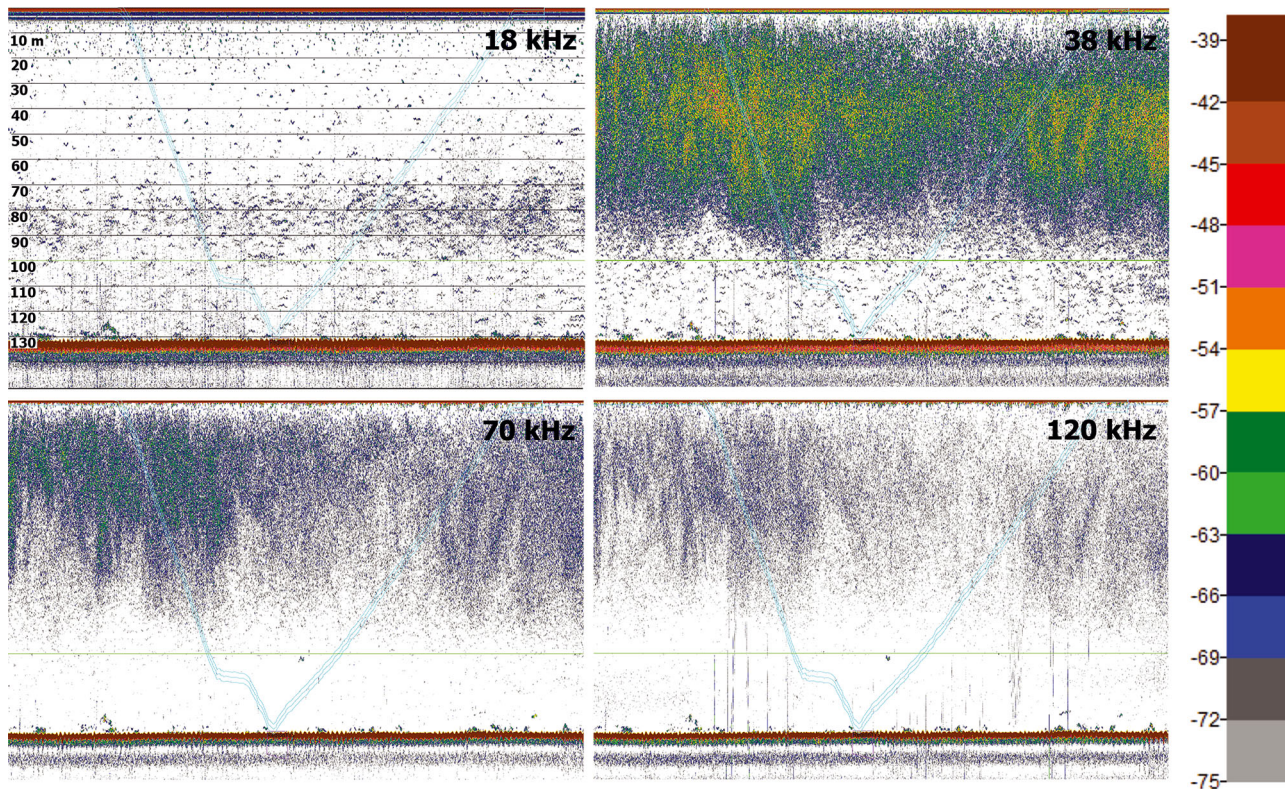


Fig. 2. Echogram (after noise removal) at 4 frequencies (18, 38, 70 and 120 kHz) recorded on 7 March 2012. The gear trajectory and the 2 parallel virtual lines (which delimited the analysis area) are represented by turquoise lines. The scale on the right indicates the volume backscattering strength (dB) in the echogram

oped at the Centre Oceanogràfic de les Balears [IEO] by J. Miquel) was used to represent the gear trajectory over the echograms in the post-processing software. The datagrams from the depth sensor towed behind the ship were thus matched to the echograms, with a file structure compatible with the Echoview version used in this work. Finally, from the gear trajectory line represented in the echograms, virtual parallel lines were generated by the Echoview software, defining the areas employed for subsequent analysis (Fig. 2).

Before any processing of the echograms, background noise was removed using the Echoview Data Generator Operator. This operator amplified the background noise at 1 m, i.e. the initial S_v value of noise, according to the formula of time-varied-gain (TVG):

$$\text{TVG} = 20 \log(R) + 2 \alpha R \quad (1)$$

where R is the depth (m) and α is the attenuation coefficient. To calculate the background noise at 1 m, a region with exclusive background noise was integrated, and its average S_v was estimated. The TVG amplification was subtracted from the $20 \log R$ echo-

grams. During the survey, the average of noise level at 1 m was -122.9 ± 3.9 (mean \pm SD), -128.2 ± 4.9 , -137.9 ± 4.9 , -140.7 ± 5.2 and -141.1 ± 4.6 dB at frequencies of 18, 38, 70, 120 and 200 kHz, respectively.

To analyse the spatial distribution of echo-intensities at the 5 frequencies employed, echo-integration measurements in terms of the nautical area scattering coefficient (NASC, in $\text{m}^2 [\text{n mile}]^{-2}$; MacLennan et al. 2002) were determined during the scrutinizing process of the echograms (Foote et al. 1991) over regions delimiting aggregations characterized as fish larvae. This characterization was based on (1) the frequency response results from the acoustic-biological data relationships; (2) the output from the Andreeva model, both approaches described below; and (3) the aggregation's shape and vertical distribution. The NASC values were averaged at an EDSU (Elementary Distance Sampling Unit; MacLennan et al. 2002) of 1 n mile and interpolated between sampling transect over the study area and mapped with Surfer® (Golden Software).

The comparative analysis of the horizontal distribution of fish larval densities and acoustic backscattering at the frequencies used was done considering

only fish larvae with a functional swimbladder. In order to estimate the density of larvae with a developed swimbladder, 7 taxa with swimbladders (*Micromesistius poutassou*, *Merluccius merluccius*, *Trisopterus minutus*, *Maurolicus muelleri*, *Sardina pilchardus*, *Trachurus trachurus* and *Callionymus* spp.) were selected from the 9 most abundant taxa; these 9 taxa represented 72% of the total fish larval community. Only hauls where the average length of larvae exceeded that of the size at which development of the swimbladder began were included in the analysis. These sizes were taken from the literature whenever possible: *M. merluccius* (Bjelland & Skiftesvik 2006), *S. pilchardus* (Ré 1986), *M. muelleri* (Ozawa 1976) and *T. trachurus* (Russell 1976). In species for which no references were found, the minimum length was taken as the mean of the length-range in the samples.

Variations in the vertical distribution patterns of larval aggregations were examined only at 38 and 70 kHz. In order to do so, the echograms obtained along the survey track were divided into 10 m depth layers, and also averaged over an EDSU of 1 n mile. The depth of layers with maximum mean S_v at each averaging point provided a reference of the depth of the aggregation core during day and night hours.

In order to determine the relationship between biological and acoustic data, linear models were fitted using R software (R Development Core Team 2014). Fish larvae abundances were \log_{10} -transformed prior to analysis to meet the assumptions of linear regression. The density of fish larvae at each depth was compared to the S_v extracted from echogram regions defined following the opening-closing time at each level. Regions were extended 4 m in height (2 m above and 2 m below the net track).

For the most dominant species, *M. poutassou*, the size of gas-bearing fish larvae at resonance was estimated following the methodology detailed by Álvarez-Colombo et al. (2011). It was performed considering the acoustic resonance response of small bubbles at the frequency range employed (Gjørseter 1977, Kloser et al. 2002, Davison et al. 2015). The size and depth at resonance for the 5 frequencies employed during the survey was determined in 2 steps: first, the Andreeva (1964) model was used to infer the size of resonant swimbladders, and then to estimate the corresponding larvae lengths we used the swimbladder-size to larval-total length relationship established for the argentine hake (*M. hubbsi*) by Álvarez-Colombo et al. (2011), assuming a similar development and inflation process on the initial life stages of these 2 gadiformes.

RESULTS

Biological sampling

Larval density pooled for all fish species ranged from 8.26 to 14400.00 larvae \times 1000 m⁻³. A total of 62 taxa (59 species and 3 genera) of larvae of 28 families were caught. The most abundant larval fish species were *Micromesistius poutassou* (accounting for 32.61% of the total larval fish density), *Scomber scombrus* (19.48%), *Trisopterus minutus* (4.49%), *Sardina pilchardus* (3.98%) *Merluccius merluccius* (3.55%) and *Trachurus trachurus* (2.69%). Larvae of *M. poutassou* and *M. merluccius* were widespread over the study area, while larvae of *S. pilchardus*, *S. scombrus*, *T. trachurus* and *T. minutus* were restricted to the shelf region (Fig. 3). Length frequency distribution of these species is shown in Fig. 4. Up to 78.7% of the total larval fish concentration was found in the upper 60 m of the water column and 92.5% in the upper 100 m. A more detailed description of the larval fish community composition and structure, horizontal and vertical distribution and diel movements of fish larvae is found in Rodríguez et al. (2015a,b).

Spatial distribution

Zooplanktonic aggregations were detected along the sampling transects. They were particularly intense at depths lower than 100 m at frequencies of 38 and 70 kHz, being higher than the acoustic threshold used during the survey (-75 kHz). The average S_v detected at 18–200 kHz ranged from -70.6 to -64.8 dB. The horizontal distribution of the densities of fish larvae with a functional swimbladder estimated from the multinet catches were compared to the acoustic backscatter distribution at all frequencies analysed. Density of fish larvae increased from south to north (Fig. 5). The main aggregation of fish larvae occurred in the northernmost area, followed by a relatively high larval fish density off A Coruña (see Fig. 1 for locations). Acoustic backscatter and density of larval fish with a swimbladder showed similar distribution patterns for all frequencies (Fig. 5). However, the best correspondences between acoustic sizes and the main larval fish aggregation was found at 38 and 70 kHz (Fig. 5c,d), while less similarity was found at the other 3 frequencies, particularly at 120 and 200 kHz (Fig. 5b,e,f).

Daytime and night-time vertical distribution of larval fish aggregations in 38 and 70 kHz echograms did not appreciably differ, particularly at 70 kHz. At

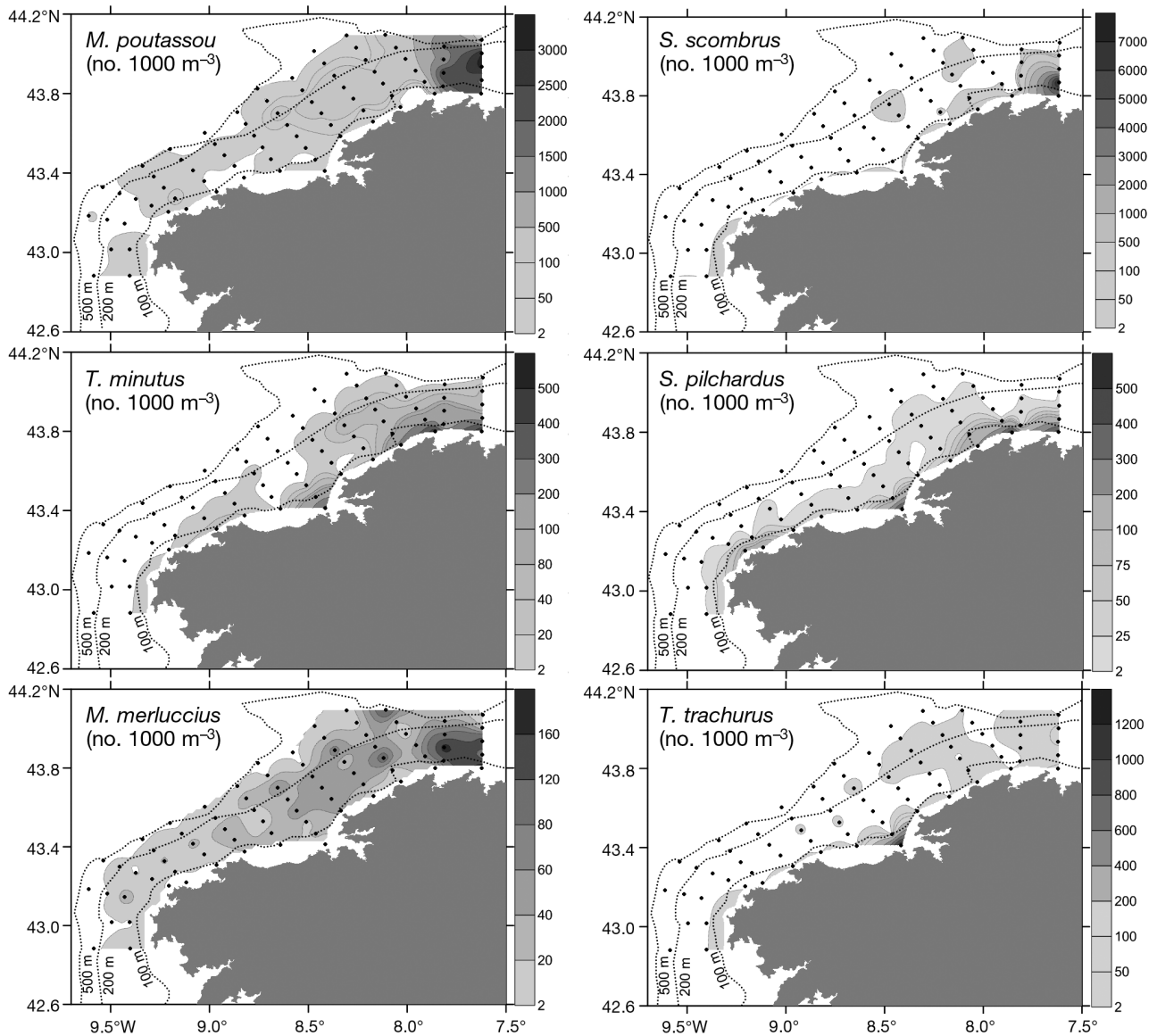


Fig. 3. Horizontal distribution of the larval fish densities (expressed as number of individuals $\times 1000 \text{ m}^{-3}$) of the 6 most abundant species collected by the MultiNet MiDi during the cruise. See 'Results' for full names of genera

38 kHz, the maximum S_v values over the surveyed area were found at depths ranging from 20 to 130 m during daylight and between 10 and 110 m depth at night (Fig. 6). However, S_v was mostly confined to between 20 and 70 m in coincidence with larval fish concentrations in net samples. A wider dispersion of the maximum acoustic values through the water column during the day and a tendency to concentrate in the shallower layers during the night, was also observed.

The depth-compensated noise levels for the frequency range used, estimated from the average recorded noise levels at 1 m, reached the mean scattering levels of the plankton layers at a minimum

depth of 190 m for 200 kHz and a maximum depth of 480 m for 38 kHz (190 and 290 m depth for the threshold of -75 dB employed, respectively). Given that those depths are greater than the maximum depth of the studied acoustic layers, the noise contribution to plankton scattering levels was considered negligible.

Relating biological sampling with acoustics

The scatterplots and linear relationships between the acoustic backscattered energy (expressed as S_v)

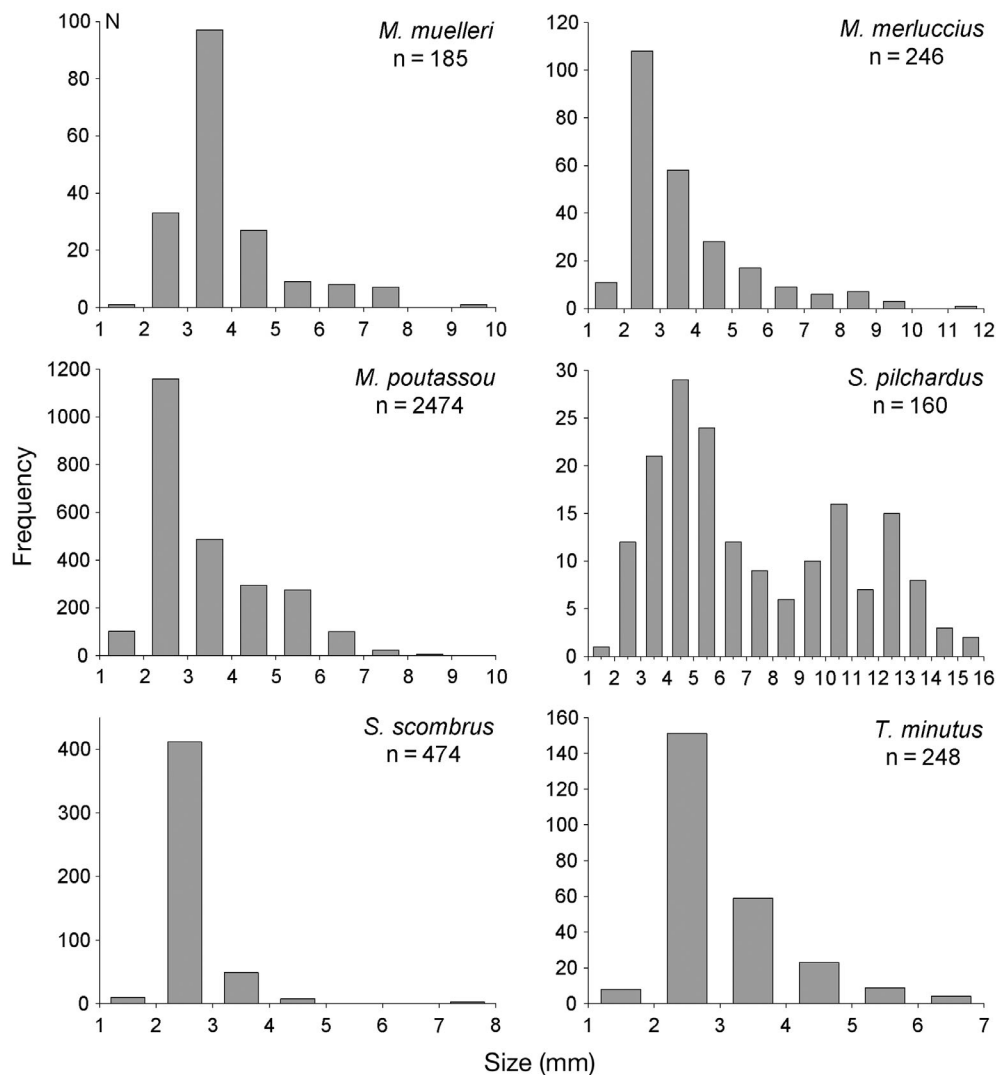


Fig. 4. Length frequency distributions (in mm) of the 6 most abundant larval fish species collected by the MultiNet MiDi during the cruise. See 'Results' for full names of genera

and density of total fish larvae are shown in Fig. 7. There was a significant relationship between S_v and density of fish larvae at all frequencies (Table 1). The best fit was obtained at 70 kHz ($R^2 = 0.577$). The regression model including fish larvae and zooplankton abundances reduced the AIC only slightly and did not increase significantly the coefficients of determination (Table 1), and actually at every frequency considered the zooplankton contribution was not significant ($p > 0.07$).

To check that swimbladders of fish larvae produced the backscatter detected by the echo sounder, we compared the S_v values to the density of all fish species that develop a swimbladder (Table 1). The regressions at each frequency yielded virtually the same results as in previous analyses and, likewise, the zooplankton abundance was not significant. Since the swimbladder inflates some time after hatching and most of the larvae collected were small

(Fig. 4), we assessed the impact of larval size on the relationship between S_v values and the density of the most abundant species, *M. poutassou*, which was also well distributed over the studied area. The linear fit improved at 38, 70 and 120 kHz when hauls with average larval length smaller than 3.0 mm were removed (Table 2). Thus, excluding those hauls, the coefficient of determination at 70 and 120 kHz was 0.526 and 0.503, respectively. When hauls with average larval length smaller than 3.5 mm were excluded, the coefficient of determination at 38 kHz was 0.428. A possible explanation may be that an inflated, i.e. functional swimbladder, can be disregarded in *M. poutassou* larvae smaller than 3.0 to 3.5 mm. The relationships slightly improved with increasing larval length at 200 kHz, whereas at 18 kHz the linear fit was not significant in every case.

In contrast, the relationship between zooplankton (fish larvae excluded) density and backscattering (S_v)

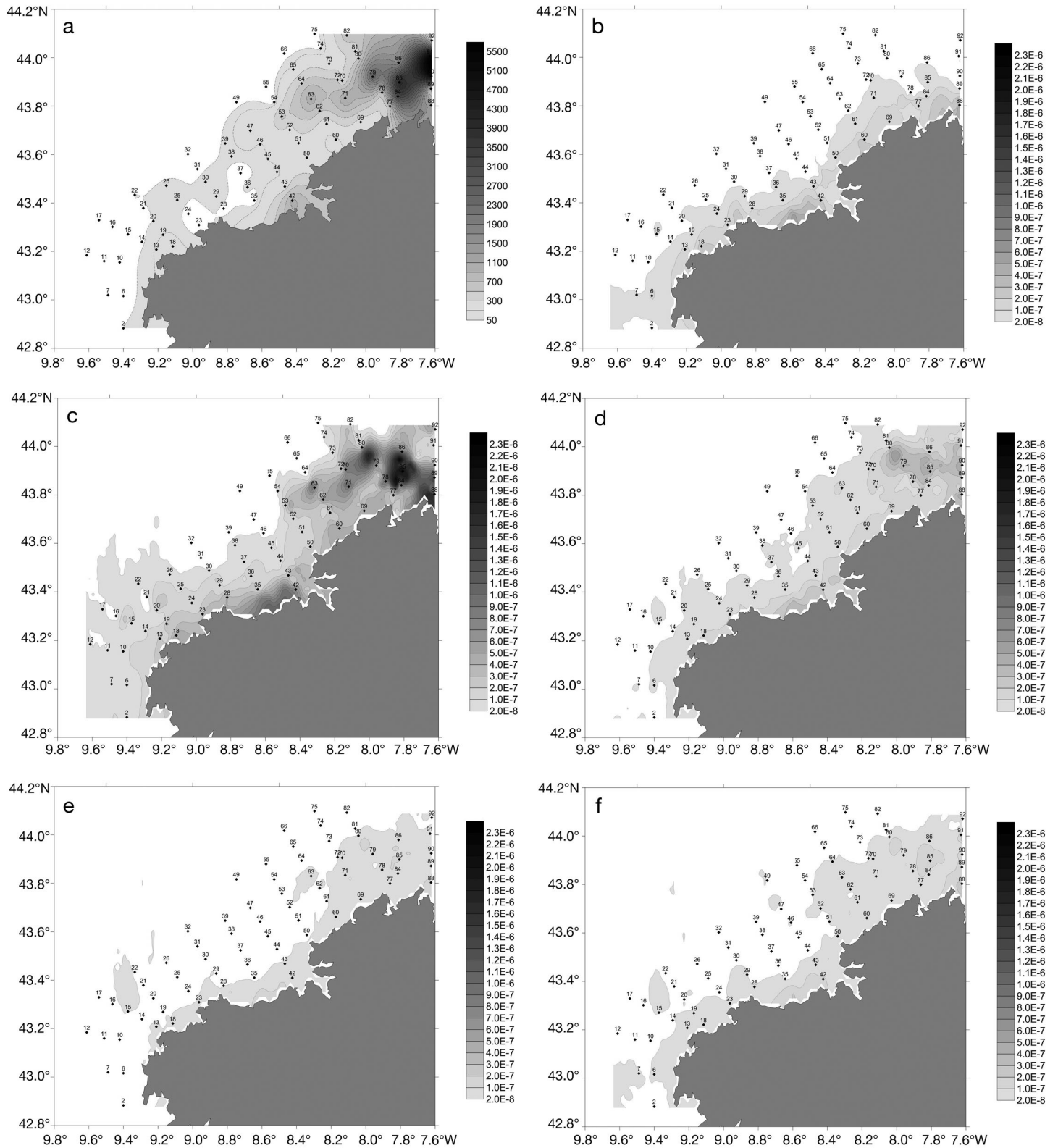


Fig. 5. Distribution maps of (a) larval fish density (in number of individuals $\times 1000 \text{ m}^{-2}$) estimated for the whole survey (considering only larvae with functional swimbladder), and acoustic backscatter (NASC; $\text{m}^2 \times \text{n mile}^{-2}$) at (b) 18 kHz, (c) 38 kHz, (d) 70 kHz, (e) 120 kHz and (f) 200 kHz

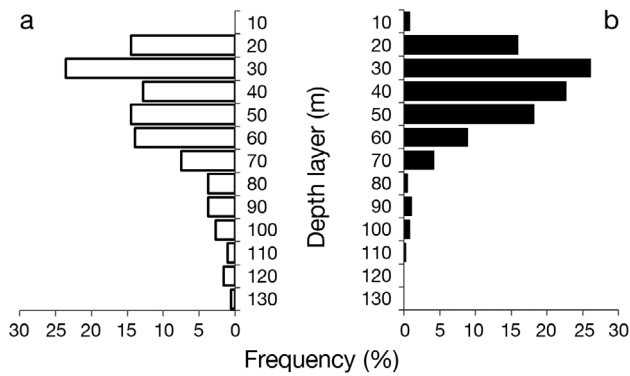


Fig. 6. Frequency of occurrence (expressed as percentage) of maximum acoustic backscattering (S_v) registered during the survey in each 10 m depth layer for (a) day and (b) night

was lower at all frequencies, not only for the total zooplankton but also for most groups (Table 3). The best fit was found for chaetognaths and polychaetes,

which reached an R^2 higher than 0.35 at 38 kHz (in the case of chaetognaths) and 70 kHz (in both groups).

For depths ranging from 20 to 70 m, a resonance is expected in 3 to 5 mm larvae of *M. poutassou* at 70 kHz and 5 to 8 mm larvae at 38 kHz. Most of the *M. poutassou* larvae caught with the plankton net fall within similar length ranges and depths. However, at frequencies of 120 to 200 kHz, resonance would be expected in larvae smaller than 3 mm, for which an inflated swimbladder in *M. poutassou* was not considered. At the lowest frequency employed (18 kHz), the models predict resonance from larvae of 10 mm and larger, which were not found in this study. In accordance, the 18 kHz echograms did not show significant echotraces in correspondence with larval fish catches, likely because the survey was completed at the beginning of the spawning season, supported by the fact that most of the larvae were in early post-hatch stages.

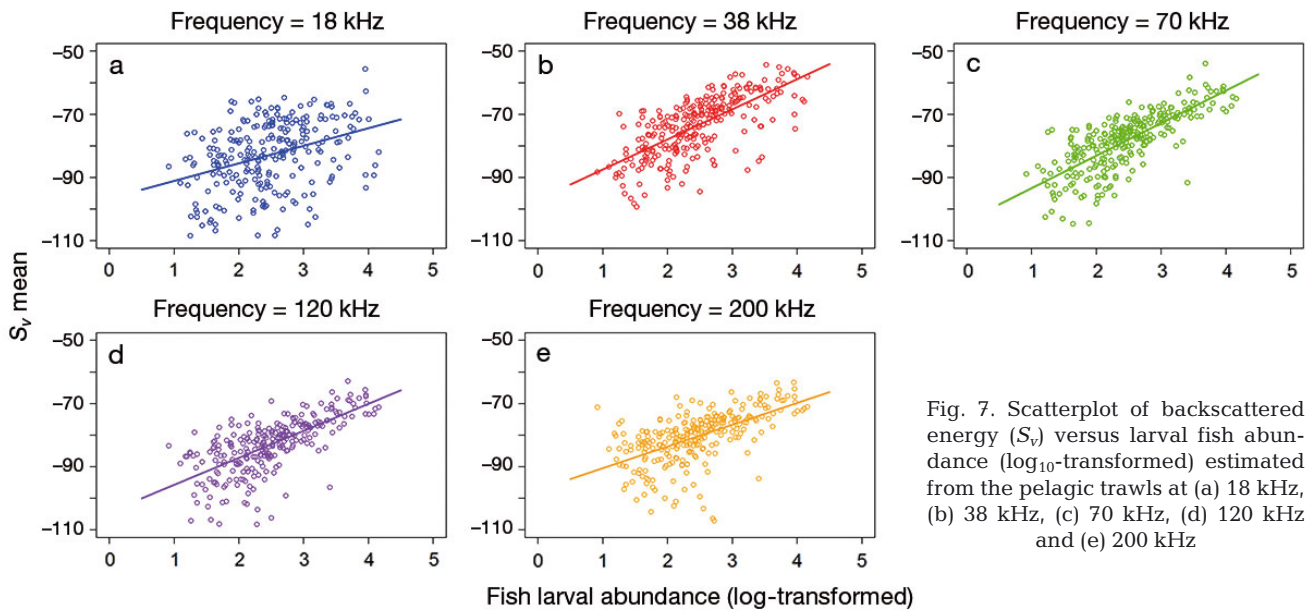


Fig. 7. Scatterplot of backscattered energy (S_v) versus larval fish abundance (\log_{10} -transformed) estimated from the pelagic trawls at (a) 18 kHz, (b) 38 kHz, (c) 70 kHz, (d) 120 kHz and (e) 200 kHz

Table 1. GLM results (Akaike information criteria [AIC] and coefficient of determination [R^2]) comparing models for testing the relationship between the acoustic backscatter (S_v) and all fish larvae abundance (FISH), abundance of fish larvae with functional swimbladder (SWFISH) and zooplankton other than fish larvae (ZOO) for each of the frequencies analysed. p-value < 0.001 for all cases

| Model | 18 kHz | | 38 kHz | | 70 kHz | | 120 kHz | | 200 kHz | |
|-------------------------|--------|-------|--------|-------|--------|-------|---------|-------|---------|-------|
| | AIC | R^2 | AIC | R^2 | AIC | R^2 | AIC | R^2 | AIC | R^2 |
| $S_v \sim$ FISH | 1893 | 0.130 | 1878 | 0.489 | 1788 | 0.577 | 1724 | 0.463 | 1814 | 0.342 |
| $S_v \sim$ FISH + ZOO | 1861 | 0.132 | 1845 | 0.489 | 1755 | 0.577 | 1691 | 0.473 | 1773 | 0.362 |
| $S_v \sim$ SWFISH | 1697 | 0.067 | 1660 | 0.381 | 1567 | 0.515 | 1520 | 0.410 | 1574 | 0.291 |
| $S_v \sim$ SWFISH + ZOO | 1668 | 0.083 | 1624 | 0.398 | 1532 | 0.527 | 1492 | 0.428 | 1540 | 0.331 |

Table 2. Coefficients of determination (Adjusted R^2) and p-values from the scatterplots of acoustic backscatter (S_v) versus *Micromesistius poutassou* larvae abundance (\log_{10} -transformed) estimated by MultiNet MiDi trawls. The inclusion or exclusion of the different hauls in these lineal regression analyses was based on the average larval lengths of *M. poutassou* for each haul

| <i>M. poutassou</i> | 18 kHz | | 38 kHz | | 70 kHz | | 120 kHz | | 200 kHz | |
|----------------------|--------|-------|--------|--------|--------|--------|---------|--------|---------|--------|
| | R^2 | p | R^2 | p | R^2 | p | R^2 | p | R^2 | p |
| Total larvae | 0.003 | 0.245 | 0.223 | <0.001 | 0.407 | <0.001 | 0.349 | <0.001 | 0.227 | <0.001 |
| Larvae \geq 2.0 mm | 0.002 | 0.275 | 0.207 | <0.001 | 0.397 | <0.001 | 0.345 | <0.001 | 0.232 | <0.001 |
| Larvae \geq 2.5 mm | 0.003 | 0.257 | 0.295 | <0.001 | 0.495 | <0.001 | 0.464 | <0.001 | 0.333 | <0.001 |
| Larvae \geq 3.0 mm | 0.016 | 0.123 | 0.409 | <0.001 | 0.526 | <0.001 | 0.503 | <0.001 | 0.314 | <0.001 |
| Larvae \geq 3.5 mm | -0.003 | 0.378 | 0.428 | <0.001 | 0.440 | <0.001 | 0.414 | <0.001 | 0.251 | <0.001 |
| Larvae \geq 4.0 mm | -0.020 | 0.945 | 0.352 | <0.001 | 0.315 | <0.001 | 0.260 | <0.001 | 0.211 | <0.001 |
| Larvae \geq 4.5 mm | -0.021 | 0.609 | 0.379 | <0.001 | 0.349 | <0.001 | 0.284 | <0.001 | 0.321 | <0.001 |

Table 3. Coefficients of determination (Adjusted R^2) and p-values from the scatterplots of acoustic backscatter (S_v) versus zooplankton (fish larvae excluded) abundance (\log_{10} -transformed) and the abundance of the different groups of zooplankton individually analysed. Abundances were estimated from MultiNet MiDi trawls

| Zooplankton group | 18 kHz | | 38 kHz | | 70 kHz | | 120 kHz | | 200 kHz | |
|-------------------|--------|--------|--------|--------|--------|--------|---------|--------|---------|--------|
| | R^2 | p | R^2 | p | R^2 | p | R^2 | p | R^2 | p |
| Total zooplankton | 0.050 | <0.001 | 0.194 | <0.001 | 0.171 | <0.001 | 0.132 | <0.001 | 0.119 | <0.001 |
| Copepods | 0.023 | <0.01 | 0.141 | <0.001 | 0.117 | <0.001 | 0.091 | <0.001 | 0.079 | <0.001 |
| Other crustaceans | 0.064 | <0.001 | 0.209 | <0.001 | 0.221 | <0.001 | 0.167 | <0.001 | 0.141 | <0.001 |
| Cnidarians | -0.003 | 0.386 | 0.008 | 0.206 | 0.010 | 0.190 | -0.012 | 0.712 | -0.003 | 0.385 |
| Molluscs | 0.114 | <0.001 | 0.249 | <0.001 | 0.218 | <0.001 | 0.170 | <0.001 | 0.169 | <0.001 |
| Chaetognaths | 0.058 | <0.001 | 0.375 | <0.001 | 0.359 | <0.001 | 0.273 | <0.001 | 0.243 | <0.001 |
| Tunicates | 0.044 | <0.001 | 0.214 | <0.001 | 0.223 | <0.001 | 0.151 | <0.001 | 0.099 | <0.001 |
| Polychaetes | 0.032 | 0.213 | 0.215 | <0.05 | 0.350 | <0.01 | 0.095 | 0.115 | 0.014 | 0.274 |
| Eggs | 0.037 | <0.01 | 0.100 | <0.001 | 0.078 | <0.001 | 0.043 | <0.001 | 0.045 | <0.001 |

DISCUSSION

Potential use of acoustic techniques and limitations

This is the first acoustic study on the larval community in Galician waters. In this paper, we compare fish larval abundance and size data collected with conventional ichthyoplankton methodology with the results of an acoustic survey at 5 frequencies. Because the acoustic backscattered energy is proportional to the number and/or size of swimbladders in fish (or gas inclusions in zooplankton), we have compared scatters to fish and zooplankton densities rather than to biomass of the individuals. The regression analyses revealed that the acoustic response at the frequency range of 38 to 120 kHz was effective in detecting larval fish aggregations. However, the predicted acoustic resonance at larval size and depth show that the 120 kHz frequency is likely ineffective in detecting fish larvae, at least for *Micromesistius poutassou* in this study. This seems to be in accordance with the lack of agreement between the larvae abundance and the

acoustic response at this frequency observed in the spatial distribution.

There are a few examples of the use of acoustics to detect fish larval aggregations at the acoustic range employed for adult fish assessments. The importance of the 38 kHz frequency for detecting *Merluccius hubbsi* larval aggregations from echograms has been previously highlighted (Álvarez-Colombo et al. (2011). Rudstam et al. (2002) found that the assessment of fish larvae smaller than 15 mm at 70 kHz was obscured due to the presence of invertebrate targets and noise. Our results indicate that the contribution of zooplankton (other than fish larvae) to total scattering at 18 to 120 kHz range in the acoustic regions corresponding with the net path was negligible, except for several groups of fluid-like zooplankton, such as chaetognaths and polychaetes. Also, the contribution of background noise was found to be low across the entire frequency range and at depths analysed

The relationships between acoustic signals and *M. poutassou* larval densities improved considerably when the stations with smaller average larval lengths were removed from the analyses. The best fits were

found when considering sizes larger than 3 to 3.5 mm, possibly related to the development of a functional swimbladder and the highest abundances at these sizes. This clearly indicates that smaller larvae did not contribute significantly to the recorded acoustic echoes. On the other hand, when considering hauls with an average size larger than 3.0 to 3.5 mm, the coefficients of determination were lower. This was likely due to the low abundance at these sizes, and then the residual noise or the contribution to total backscattering from other organisms may contribute more to the acoustic signals.

The time, and hence larval size, of the swimbladder's first inflation is species-specific. For example swimbladder formation in *Trachurus trachurus* occurs at 4 mm standard length (Russell 1976), in *Engraulis encrasicolus* at 7 mm and in *Sardina pilchardus* at 10 mm (Ré 1986). Thus, it is critical to study the ontogeny of swimbladder inflation for the construction of backscattering models used to interpret acoustic surveys (Davison 2011). Our results suggest that the development of a functional swimbladder in *M. poutassou* occurs at a length of 3.0 to 3.5 mm standard length, slightly smaller than that observed for other Gadiformes, such as *M. hubbsi* (Álvarez-Colombo et al. 2011) and *Merluccius merluccius* (Bjelland & Skiftesvik 2006).

As contrasting examples, while the detection and analysis of *M. hubbsi* larvae on the Argentinean shelf is carried out in a rather straightforward manner, given the low larval species diversity and the enormous abundances of all larval stages of *M. hubbsi* during its reproductive season (Álvarez-Colombo et al. 2011), in Galician waters this constitutes a complex task because of the relatively high diversity of the larval fish assemblage in this region. Nevertheless, the high abundance of resonant fish larvae, particularly *M. poutassou*, provided an opportunity to isolate and map the spatial distribution of their aggregations over the entire survey.

The scrutinizing process employed in interpreting the survey datasets implies that the user, not the system, makes all the important decisions in the course of interpreting the data, as denoted by Foote et al. (1991). This methodology is inherently subjective, as this involves making decisions about the nature of scatterers from an under-dimensioned graphical representation and based on the operator's experience (Foote et al. 1991, Godø et al. 2004). However, auxiliary data provided by the post-processing software (TS distribution, NASC relative frequency response) and other features contribute to the interpretation criterion.

Although the MultiNet MiDi allows the study of the vertical distribution of fish larvae (Rodríguez et al. 2015b), it is normally assumed that there will be some degree of avoidance of this sampler from the larger fraction of the actual larval length range. However, our survey was completed at the beginning of the spawning season, with most caught larvae being in early post-hatch stages. Consequently, most larvae captured in this study were early-stage larvae with little ability to avoid the net. Also, our models predicted a resonance from larvae of 10 mm length or more at the frequency of 18 kHz, but the related echograms did not show significant echotraces in correspondence with larval fish catches. This suggests that larvae of these sizes were not present in the study area at the time of sampling.

In environments characterized by multi-specific assemblages of acoustic targets, detecting and isolating the different acoustic signals requires advanced multi-frequency acoustic techniques, allowing for the classification of echotraces and scattering layers into species or species groups with distinct scattering properties (Korneliussen & Ona 2002, 2003). The contribution of acoustic targets other than fish larvae to the total scattering recorded at the different frequencies employed has not been determined in this preliminary study, focused as it was on the detection of resonant fish larvae at a frequency range where the contribution of other zooplankton taxa was negligible. However, multifrequency acoustic techniques should be included in future research to study in detail the complexity of zooplankton community structure in Galician waters.

The present study emphasizes the application of echo-sounding data obtained at frequencies routinely used during research cruises and also during vessels of opportunity operations which could extend the spatial and temporal coverage of acoustic data collection beyond those of research vessel programs (Dalen & Karp 2007). Also, the acoustic characterization of fish larval aggregations at narrow-band, commonly employed frequencies provides an available methodology for the study of trends in the distribution and relative abundance of fish larvae in existent acoustic databases.

Implications of the results in recruitment and fisheries management

The poorly defined stock–recruitment relationship is a cornerstone of fisheries assessment and management via projected stock development and inher-

ently in biological reference points (Saborido-Rey & Trippel 2013). The understanding of recruitment variability has been improved in recent decades through the concept of stock reproductive potential (Trippel 1999, Saborido-Rey & Trippel 2013) intimately linked to larval survivorship through the parental effects on larval viability (Kamler 2005, Green 2008). Field applications of these results have been prevented by the inherent difficulty of getting proper data on larval distribution and abundance to conduct correlation analyses (Lo et al. 2009). Yet, recruitment in fish populations is largely determined during the early life-history stages by a combination of factors operating over multiple spatio-temporal scales such as predation, starvation, and spatial mismatch with appropriate areas for survival (Leggett & DeBlois 1994, Subbey et al. 2014) and references therein). Despite some advances, it remains difficult to obtain accurate and precise estimates of abundance of early life-history stages of fishes, their predators, and prey at the spatial scales over which they interact (Houde 2009).

With the potential of acoustic methodology, improved studies can be conducted to test with highest confidence the enduring theories and hypotheses on recruitment fluctuations (reviewed by Houde 2009 and Hare 2014). In particular, this has applications for (1) observing the density-dependent interactions between fish larvae and their predators and prey, (2) determining the drivers and factors affecting movement and distributional patterns of fish larvae, (3) building and assessing quantitative drift models, pairing them with the high-resolution ocean circulation models developed in past decades (Staaterman & Paris 2014), (4) understanding the underlying processes determining the timing and duration of the recruitment interval, which is critical for assessment of the impact of specific mortality, (5) studying habitat selection and consequently a better estimation of recruitment at the stage of pre-settlement, and finally (6) estimating the spawning biomass using larval production methods, especially when fish eggs are not available or accessible, or are difficult to identify (Lo et al. 2009).

CONCLUSIONS

This study shows that larval aggregations in Galician waters can be detected and quantified with a relative abundance index derived from acoustic methods. Abundance of fish larvae with a swimbladder estimated with acoustics was comparable and

correlated with that obtained from conventional sampling methods, particularly at 38 and 70 kHz. Thus, in this time of technological advancement, acoustics appear to be a useful tool in overcoming difficulties associated with studies of larval ecology and fish recruitment.

Acknowledgements. The authors thank the crew of RV 'Cornide de Saavedra' and all the participants in the Cramer 0312 cruise for their assistance. This work was supported by the project CRAMER (CTM2010-21856-CO3), funded by the Spanish Ministry of Economy and Competitiveness and by the project ECOPREGA (10MMA602021PR), funded by the Regional Government of Galicia (Xunta de Galicia). We are also grateful to the 2 anonymous referees for their constructive comments on the manuscript.

LITERATURE CITED

- Aiken CM, Navarrete SA (2011) Environmental fluctuations and asymmetrical dispersal: generalized stability theory for studying metapopulation persistence and marine protected areas. *Mar Ecol Prog Ser* 428:77–88
- Almany GR, Connolly SR, Heath DD, Hogan JD and others (2009) Connectivity, biodiversity conservation and the design of marine reserve networks for coral reefs. *Coral Reefs* 28:339–351
- Álvarez P, Chifflet M (2012) The fate of eggs and larvae of three pelagic species, mackerel (*Scomber scombrus*), horse mackerel (*Trachurus trachurus*) and sardine (*Sardina pilchardus*) in relation to prevailing currents in the Bay of Biscay: Could they affect larval survival? *Sci Mar* 76:573–586
- Álvarez-Colombo G, Dato C, Macchi GJ, Palma E and others (2011) Distribution and behavior of Argentine hake larvae: Evidence of a biophysical mechanism for self-recruitment in northern Patagonian shelf waters. *Cienc Mar* 37:633–657
- Andreeva IB (1964) Scattering of sound by air bladders of fish in deep sound-scattering ocean layers. *Sov Phys Acoust* 10:17–20
- Bachiller E, Fernandes JA (2011) Zooplankton image analysis manual: automated identification by means of scanner and digital camera as imaging devices. *Rev Invest Mar* 18:16–37
- Bachiller E, Fernandes JA, Irigoien X (2012) Improving semiautomated zooplankton classification using an internal control and different imaging devices. *Limnol Oceanogr Methods* 10:1–9
- Barkley RA (1972) Selectivity of towed-net samplers. *Fish Bull* 70:799–820
- Beaugrand G, Brander KM, Lindley JA, Souissi S, Reid PC (2003) Plankton effect on cod recruitment in the North Sea. *Nature* 426:661–664
- Becker BJ, Levin LA, Fodrie FJ, McMillan PA (2007) Complex larval connectivity patterns among marine invertebrate populations. *Proc Natl Acad Sci USA* 104:3267–3272
- Bjelland RM, Skiftesvik AB (2006) Larval development in European hake (*Merluccius merluccius* L.) reared in a semi-intensive culture system. *Aquacult Res* 37:1117–1129

- Bonanno A, Goncharov S, Mazzola S, Popov S and others (2006) Acoustic evaluation of anchovy larvae distribution in relation to oceanography in the Cape Passero area (Strait of Sicily). *Chem Ecol* 22:S265–S273
- Cowen RK, Sponaugle S (2009) Larval dispersal and marine population connectivity. *Annu Rev Mar Sci* 1:443–466
- Cowen RK, Paris CB, Srinivasan A (2006) Scaling of connectivity in marine populations. *Science* 311:522–527
- Dalen J, Karp WA (2007) Collection of acoustic data from fishing vessels. ICES, Copenhagen, Coop Res Rep No. 287
- Davison P (2011) The specific gravity of mesopelagic fish from the northeastern Pacific Ocean and its implications for acoustic backscatter. *ICES J Mar Sci* 68:2064–2074
- Davison P, Lara-Lopez A, Koslow JA (2015) Mesopelagic fish biomass in the southern California current ecosystem. *Deep-Sea Res II* 112:129–142
- Fariña AC, Freire J, González-Gurriarán E (1997) Demersal fish assemblages in the Galician continental shelf and upper slope (NW Spain): spatial structure and long-term changes. *Estuar Coast Shelf Sci* 44:435–454
- Foote KG, Knudsen HP, Vestnes G (1987) Calibration of acoustic instruments for fish density estimation: a practical guide. ICES, Copenhagen, Coop Res Rep No. 144
- Foote KG, Knudsen HP, Korneliussen RJ, Nordbø PE, Røang K (1991) Postprocessing system for echo sounder data. *J Acoust Soc Am* 90:37–47
- Gjøsaeter J (1977) Aspects of the distribution and ecology of the Myctophidae from the Western and Northern Arabian Sea. Indian Ocean Fishery and Development Programme: Pelagic Fish Assessment Survey North Arabian Sea
- Godø OR, Hjellvik V, Greig T, Beare D (2004) Can subjective evaluation of echograms improve correlation between bottom trawl and acoustic densities? *ICES CM* 2004 R:23
- Godø OR, Patel R, Pedersen G (2009) Diel migration and swimbladder resonance of small fish: some implications for analyses of multifrequency echo data. *ICES J Mar Sci* 66:1143–1148
- Godø OR, Handegard NO, Browman HI, Macaulay GJ and others (2014) Marine ecosystem acoustics (MEA): quantifying processes in the sea at the spatio-temporal scales on which they occur. *ICES J Mar Sci* 71:2357–2369
- Green BS (2008) Maternal effects in fish populations. *Adv Mar Biol* 54:1–105
- Hare JA (2014) The future of fisheries oceanography lies in the pursuit of multiple hypotheses. *ICES J Mar Sci* 71:2343–2356
- Hernandez FJ Jr, Carassou L, Muffelman S, Powers SP, Graham WM (2011) Comparison of two plankton net mesh sizes for ichthyoplankton collection in the northern Gulf of Mexico. *Fish Res* 108:327–335
- Hjort J (1914) Fluctuations in the great fisheries of northern Europe viewed in the light of biological research. Proc Rapports et Procès-Verbaux des Réunions du Conseil International pour l'Exploration de la Mer. ICES, Copenhagen, p 228
- Houde ED (2008) Emerging from Hjort's shadow. *J Northwest Atl Fish Sci* 41:53–70
- Houde ED (2009) Recruitment variability. In: Jakobsen T, Fogarty MJ, Megrey BA, Moksness E (eds) Fish reproductive biology: implications for assessment and management. Wiley-Blackwell, Oxford, p 91–171
- Ibaibarriaga L, Irigoien X, Santos M, Motos L and others (2007) Egg and larval distributions of seven fish species in north-east Atlantic waters. *Fish Oceanogr* 16:284–293
- Johnson DL, Morse WW (1994) Net extrusion of larval fish: correction factors for 0.333 mm versus 0.505 mm mesh bongo nets. *NAFO Sci Counc Studies* 20:85–92
- Kamler E (2005) Parent–egg–progeny relationships in teleost fishes: an energetics perspective. *Rev Fish Biol Fish* 15:399–421
- Kloser RJ, Ryan T, Sakov P, Williams A, Koslow JA (2002) Species identification in deep water using multiple acoustic frequencies. *Can J Fish Aquat Sci* 59:1065–1077
- Korneliussen RJ, Ona E (2002) An operational system for processing and visualizing multi-frequency acoustic data. *ICES J Mar Sci* 59:293–313
- Korneliussen RJ, Ona E (2003) Synthetic echograms generated from the relative frequency response. *ICES J Mar Sci* 60:636–640
- Le Corre N, Guichard F, Johnson LE (2012) Connectivity as a management tool for coastal ecosystems in changing oceans. In: Marcelli M (ed) *Oceanography*. InTech Open Access Publisher, Rijeka, p 235–258
- Leggett WC, Deblois E (1994) Recruitment in marine fishes: Is it regulated by starvation and predation in the egg and larval stages? *Neth J Sea Res* 32:119–134
- Leslie JK, Timmins CA (1989) Double nets for mesh aperture selection and sampling in ichthyoplankton studies. *Fish Res* 7:225–232
- Lo NCH, Smith PE, Takahashi M (2009) Egg, larval, and juvenile surveys. In: Jakobsen T, Fogarty MJ, Megrey BA, Moksness E (eds) *Fish reproductive biology: implications for assessment and management*. Wiley-Blackwell, Oxford, p 207–229
- MacLennan DN, Holliday DV (1996) Fisheries and plankton acoustics: past, present, and future. *ICES J Mar Sci* 53:513–516
- MacLennan DN, Fernandes PG, Dalen J (2002) A consistent approach to definitions and symbols in fisheries acoustics. *ICES J Mar Sci* 59:365–369
- McClain CR, Chao SY, Atkinson LP, Blanton JO, De Castillejo F (1986) Wind-driven upwelling in the vicinity of Cape Finisterre, Spain. *J Geophys Res Oceans* 91:8470–8486
- Misund OA (1997) Underwater acoustics in marine fisheries and fisheries research. *Rev Fish Biol Fish* 7:1–34
- Miyashita K (2003) Diurnal changes in the acoustic-frequency characteristics of Japanese anchovy (*Engraulis japonicus*) post-larvae 'shirasu' inferred from theoretical scattering models. *ICES J Mar Sci* 60:532–537
- Motos L, Uriarte A, Valencia V (1996) The spawning environment of the Bay of Biscay anchovy (*Engraulis encrasicolus* L.). *Sci Mar* 60:117–140
- Nielsen TG, Munk P (1998) Zooplankton diversity and the predatory impact by larval and small juvenile fish at the Fisher Banks in the North Sea. *J Plankton Res* 20:2313–2332
- Ozawa T (1976) Early life history of the Gonostomatid fish, *Pollichthys maui*, in the oceanic region off Southern Japan. *Jpn J Ichthyol* 23:43–54
- Pusack TJ, Christie MR, Johnson DW, Stallings CD, Hixon MA (2014) Spatial and temporal patterns of larval dispersal in a coral-reef fish metapopulation: evidence of variable reproductive success. *Mol Ecol* 23:3396–3408
- R Development Core Team (2014) R: a language and environment for statistical computing. R Foundation for Statistical Computing, Vienna. www.r-project.org

- Ré P (1986) Otolith microstructure and the detection of life history events in sardine and anchovy larvae. *Cienc Biol Ecol Syst* 6:9–17
- Rodriguez JM, Cabrero A, Gago J, Garcia A, Laiz-Carrión R, Piñeiro C, Saborido-Rey F (2015a) Composition and structure of the larval fish community in the NW Iberian upwelling system during the winter mixing period. *Mar Ecol Prog Ser* 533:245–260
- Rodriguez JM, Cabrero A, Gago J, Guevara-Fletcher C and others (2015b) Vertical distribution and migration of fish larvae in the NW Iberian upwelling system during the winter mixing period: implications for cross-shelf distribution. *Fish Oceanogr* 24:274–290
- Rudstam LG, VanDeValk AJ, Scheuerell MD (2002) Comparison of acoustic and Miller high-speed sampler estimates of larval fish abundance in Oneida Lake, New York. *Fish Res* 57:145–154
- Russell FS (1976) The eggs and planktonic stages of British marine fishes. Academic Press, London
- Saborido-Rey F, Trippel EA (2013) Fish reproduction and fisheries. *Fish Res* 138:1–4
- Staaterman E, Paris CB (2014) Modelling larval fish navigation: the way forward. *ICES J Mar Sci* 71:918–924
- Stratoudakis Y, Bernal M, Uriarte A (2004) The DEPM estimation of spawning-stock biomass for sardine and anchovy. ICES, Copenhagen, Coop Res Rep No. 268
- Subbey S, Devine JA, Schaarschmidt U, Nash RDM (2014) Modelling and forecasting stock–recruitment: current and future perspectives. *ICES J Mar Sci* 71:2307–2322
- Surís-Regueiro JC, Santiago JL (2014) Characterization of fisheries dependence in Galicia (Spain). *Mar Policy* 47:99–109
- Theilacker GH (1980) Changes in body measurements of larval northern anchovy, *Engraulis mordax*, and other fishes due to handling and preservation. *Fish Bull* 78:685–692
- Trippel EA (1999) Estimation of stock reproductive potential: history and challenges for Canadian Atlantic gadoid stock assessments. *J Northwest Atl Fish Sci* 25:61–82
- Van der Lingen CD, Huggett JA (2003) The role of ichthyoplankton surveys in recruitment research and management of South African anchovy and sardine. In: Browman HI, Skiftesvik AB (eds) *The big fish bang: Proc 26th Annu Larval Fish Conf*. Institute of Marine Research, Bergen, p 303–343
- Wiebe PH, Boyd SH, Davis BM, Cox JL (1982) Avoidance of towed nets by the euphausiid *Nematoscelis megalops*. *Fish Bull* 80:75–91

Editorial responsibility: Alejandro Gallego, Aberdeen, UK

*Submitted: June 3, 2015; Accepted: March 30, 2016
Proofs received from author(s): May 21, 2016*